A computational model of mitochondrial deoxynucleotide metabolism and DNA replication

Patrick C. Bradshaw and David C. Samuels

Am J Physiol Cell Physiol 288:989-1002, 2005. First published Jan 5, 2005;
doi:10.1152/ajpcell.00530.2004

AJP - Cell Physiology is dedicated to innovative approaches to the study of cell and molecular physiology. It is published 12 times a year (monthly) by the American Physiological Society, 9650 Rockville Pike, Bethesda MD 20814-3991. ISSN: 0363-6143, ESSN: 1522-1563. Visit our website at http://www.the-aps.org/.

Am J Physiol Cell Physiol 288: C989–C1002, 2005.
First published January 5, 2005; doi:10.1152/ajpcell.00530.2004.

A computational model of mitochondrial deoxynucleotide metabolism and DNA replication

Patrick C. Bradshaw and David C. Samuels

Virginia Bioinformatics Institute, Virginia Polytechnic and State University, Blacksburg, Virginia

Submitted 29 October 2004; accepted in final form 30 December 2004

Bradshaw, Patrick C., and David C. Samuels. A computational model of mitochondrial deoxynucleotide metabolism and DNA replication. *Am J Physiol Cell Physiol* 288: C989–C1002, 2005. First published January 5, 2005; doi:10.1152/ajpcell.00530.2004.—We present a computational model of mitochondrial deoxynucleotide metabolism and mitochondrial DNA (mtDNA) synthesis. The model includes the transport of deoxynucleosides and deoxynucleotides into the mitochondrial matrix space, as well as their phosphorylation and polymerization into mtDNA. Different simulated cell types (cancer, rapidly dividing, slowly dividing, and postmitotic cells) are represented in this model by different cytoplasmic deoxynucleotide concentrations. We calculated the changes in deoxynucleotide concentrations within the mitochondrion during the course of a mtDNA replication event and the time required for mtDNA replication in the different cell types. On the basis of the model, we define three steady states of mitochondrial deoxynucleotide metabolism: the phosphorylating state (the net import of deoxynucleosides and export of phosphorylated deoxynucleotides), the desphosphorylating state (the reverse of the phosphorylating state), and the efficient state (the net import of both deoxynucleosides and deoxynucleotides). We present five testable hypotheses based on this simulation. First, the deoxynucleotide pools within a mitochondrion are sufficient to support only a small fraction of even a single mtDNA replication event. Second, the mtDNA replication time in postmitotic cells is much longer than that in rapidly dividing cells. Third, mitochondria in dividing cells are net sinks of cytoplasmic deoxynucleotides, while mitochondria in postmitotic cells are net sources. Fourth, the deoxynucleotide carrier exerts the most control over the mtDNA replication rate in rapidly dividing cells, but in postmitotic cells, the NDPK and TK2 enzymes have the most control. Fifth, following from the previous hypothesis, rapidly dividing cells derive almost all of their mtDNA precursors from the cytoplasmic deoxynucleotides, not from phosphorylation within the mitochondrion.

simulation; nucleotide phosphorylation; nucleoside transport; mitochondrial DNA

THE HUMAN MITOCHONDRIAL GENOME is a circular molecule encoding 13 peptides, 22 tRNAs, and 2 rRNAs. The mammalian mitochondrial genome is highly compact, consisting of only ~17,000 bp. Even though mammalian cells typically contain thousands of copies of the mitochondrial genome, <1% of total cellular DNA is contained inside the mitochondria.

Mitochondrial DNA (mtDNA) replication occurs during all phases of the cell cycle, even in postmitotic cells in which nuclear DNA synthesis has ceased. The measured half-life of mtDNA in mammalian cells is 10–30 days (25). Without this ongoing process of mtDNA replication and the nucleotide metabolism supporting replication, mtDNA depletion occurs rapidly, eventually disrupting the production of ATP and causing failure of the cell to function. Errors in the mitochondrial nucleotide metabolism also can be a cause of mtDNA mutations by changing the balance of the four deoxynucleotide triphosphate pools in the mitochondrion (72). Many genetic diseases characterized by mtDNA depletion or increased mtDNA mutation rates are caused by mutations in the nuclear genes for enzymes of nucleotide metabolism (48). To understand these diseases, we must first understand normal mitochondrial deoxynucleotide metabolism. In this paper, we describe a computational model of the deoxynucleotide metabolism within an individual mitochondrion, coupled to the deoxynucleotides and deoxynucleosides within the cytoplasm.

Transport and phosphorylation of mtDNA precursors. The mitochondrion is surrounded by a double membrane defining two separate compartments within the organelle: the intermembrane space between the outer and inner membranes and the matrix space within the inner membrane. The mtDNA molecules are located within the matrix space. The outer membrane is highly porous to all nucleosides and nucleotides; therefore, we consider the intermembrane space to be in equilibrium with the cell cytoplasm and do not consider it a separate compartment in the model. The mitochondrial inner membrane is highly impermeable to solutes, so specific transporters are located there to provide the precursors needed for mtDNA synthesis (Fig. 1). The inner membrane contains at least two proteins that transport DNA precursors into the mitochondrial matrix: the deoxynucleotide carrier (DNC) and an equilibrative nucleoside transporter (ENT). The DNC has been reported to transport deoxynucleotide diphosphates (dNDPs) into the mitochondrial matrix in exchange for ADP or ATP (13). The DNC also transports deoxynucleotide triphosphates (dNTPs), but less efficiently than dNDPs. In humans, hENT1 has been identified as a mitochondrial deoxynucleoside (dN) transporter (40). In addition to this general nucleoside transporter, a dN transporter specific for deoxyguanosine has been reconstituted from rat liver mitochondria (83). To summarize, mitochondrial deoxynucleotide metabolism is connected to cytoplasmic deoxynucleotide metabolism at both ends of the phosphorylation process: at the deoxynucleoside level and at the diphosphate and triphosphate levels.

Once transported into the mitochondrial matrix space, deoxynucleosides must be phosphorylated to the triphosphate form to be incorporated into mtDNA. Two irreversible enzymes, deoxyguanosine kinase (dGK) for purines and thymidine kinase 2 (TK2) for pyrimidines, catalyze the first phosphorylation step (18). Mitochondrial nucleotidase enzymes remove the phosphate group (61, 63) from the deoxynucleotide

Address for reprint requests and other correspondence: D. C. Samuels, Virginia Bioinformatics Institute, Virginia Polytechnic and State Univ., Bioinformatics Facility I (0477), Blacksburg, VA 24061 (E-mail: dsamuels@vbi.vt.edu).

The costs of publication of this article were defrayed in part by the payment of page charges. The article must therefore be hereby marked "*advertisement*" in accordance with 18 U.S.C. Section 1734 solely to indicate this fact.

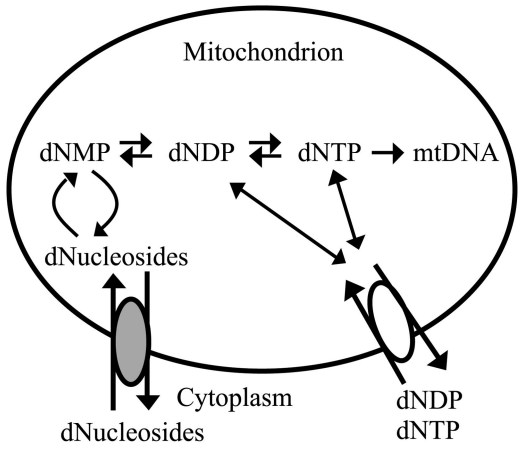

Fig. 1. Schematic showing general deoxynucleotide metabolism in a mitochondrion. dNMP, deoxynucleotide monophosphate; dNDP, deoxynucleotide diphosphate; dNTP, deoxynucleotide triphosphate; mtDNA, mitochondrial DNA.

monophosphate (dNMP) molecules. The combined action of these enzymes forms a futile substrate cycle (Figs. 1 and 2). Separate nucleoside monophosphate kinases (NMPKs) for dAMP, dCMP, dGMP, and dTMP are thought to exist to catalyze the second phosphorylation step and are reversible enzymes. The final phosphorylation uses the reversible nucleoside diphosphate kinase (NDPK) enzyme for all dNDP and ribonucleotide NDP substrates. Human isoforms nm23-h4 and nm23-h6 may perform this function (39). A diagram of the enzymes and substrates of the phosphorylation pathway is shown in Fig. 2. Material can enter or leave this chain of phosphorylation steps at the nucleoside level, the diphosphate level, or the triphosphate level. Only the monophosphate level is directly isolated from the cytoplasm. Unlike many cytoplasmic enzymes involved in deoxynucleotide metabolism, the corresponding mitochondrial enzymes are not differentially regulated throughout the cell cycle (13, 18).

Interactions between ribonucleotide and deoxyribonucleotide metabolism. Because mitochondria apparently do not possess ribonucleotide reductase for de novo deoxynucleotide synthesis from ribonucleotides, mitochondrial ribonucleotide and deoxyribonucleotide metabolism are not directly linked. However, many mitochondrial enzymes accept both ribonucleotide and deoxyribonucleotide substrates. Therefore, competition for the enzymes may limit the accessibility of deoxynucleotide substrates, because these substrates are generally present in much lower quantities than are ribonucleotides. The monophosphate kinases for dAMP, dCMP, and dGMP have been shown or are thought to compete with ribonucleotides on the basis of their cytoplasmic counterparts (Table 1). Mitochondrial NDPK also uses ribo- as well as deoxyribonucleotides as substrates. We have included these inhibitions in the model. Evidence has been presented that the mtDNA polymerase-γ incorporates ribonucleotides into mtDNA (85), so NTPs may compete with dNTPs for polymerase-γ, although we have not included that inhibitor in this model.

Mitochondrial polymerase-γ. Mitochondrial polymerase-γ is the only DNA polymerase located in metazoan mitochondria. The polymerase-γ holoenzyme is composed of a catalytic subunit and an accessory subunit that binds DNA and increases the processivity of the enzyme (9). In vitro, with high dNTP concentrations, the mitochondrial polymerase-γ holoenzyme can extend a DNA template at a rate of nearly 40 deoxynucleotides per second (34), corresponding to a replication time of 7 min per mitochondrial genome (assuming 2 polymerases operating simultaneously per mtDNA molecule). However, in situ, it takes 60–120 min to completely replicate the ~33,000 bp in this genome (6). Relatively slow helicase activity (37) or limiting mitochondrial deoxynucleotides may be responsible for the slower polymerization rate in situ. The generally quoted replication time of 1–2 h was measured in rapidly dividing cells in cell culture. Our simulation results show that the mtDNA replication time may depend strongly on cell type.

MtDNA replication. With 2–10 mtDNA molecules per organelle and ~1 h required for mtDNA synthesis in rapidly dividing cells (which must double their mtDNA content during the cell division period of ~24 h), mtDNA replications most likely occur as individual events, with only one mtDNA molecule replicating at any one time within a single mitochondrion and often with no molecules replicating in the organelle. Slowly dividing or postmitotic cells are even less likely to have overlapping mtDNA replication events in a single mitochondrion. So, we may consider individual, nonoverlapping mtDNA replication events to be the normal situation.

The two strands of the mtDNA molecule are called the heavy and light strands because of a large imbalance in guanine between the two strands. Two distinct models have been proposed for mtDNA replication. In the classic Clayton-Vinograd model, mtDNA replication occurs through an asynchronous displacement mechanism using an origin of replication for the heavy strand of mtDNA (O_H) and a separate origin of replication for the light strand (O_L) (6). The O_H is located in the displacement loop (D-loop) of mtDNA, a short stretch of ~1,000 nucleotides that often contains single-stranded DNA adjacent to the duplex DNA. According to this asynchronous

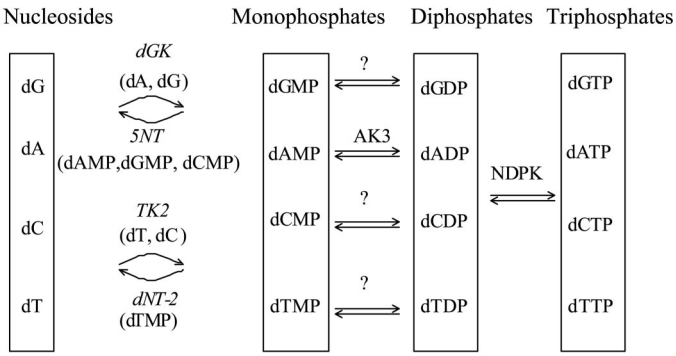

Fig. 2. Nucleotide phosphorylation in mitochondria. Enzymes are listed followed by substrates in parenthesis. Enzymes for which a specific gene has not been identified are indicated by question marks. dG, deoxyguanosine; dGK, deoxyguanosine kinase; dGMP, deoxyguanosine monophosphate; dGDP, deoxyguanosine diphosphate; dGTP, deoxyguanosine triphosphate; dA, deoxyadenosine; 5NT, 5′-nucleotidase; dAMP, deoxyadenosine monophosphate; dCMP, deoxycytidine monophosphate; AK3, adenylate kinase 3; NDPK, nucleoside diphosphate kinase; dC, deoxycytidine; TK2, thymidine kinase 2; dCDP, diphosphate; dCTP, dicytidine triphosphate; dT, deoxythymidine; dNT-2, deoxynucleotidase 2; dTMP, deoxythymidine monophosphate; dTDP, deoxythymidine diphosphate; dTTP, deoxythymidine triphosphate.

Table 1. *Substrates and inhibitors of mitochondrial deoxynucleotide metabolism*

Enzyme	Substrates and Inhibitors (K_i), μM (Ref.)	Description
TK2	dT (4.9) (82), dC (40) (82), dTTP (2.3) (83), dCTP (0.83) (82)	Nucleoside kinase; catalyzes first phosphorylation
dGK	dG, dA, dGMP (4) (29), dAMP (28) (29), dGTP (0.4) (29), dATP (41) (29)	Nucleoside kinase; catalyzes first phosphorylation
dNT-2	dTMP	Nucleotidase
5′-NT*	dAMP, dCMP, dGMP, *AMP* (94) (61), *ADP* (1,400) (61), *ATP* (660) (61)	Nucleotidase
Mt-TMPK*	dTMP, dTDP	Second phosphorylation step; reversible enzyme
Mt-UMP-CMP kinase*	dCMP, dCDP, *CMP* (23) (10), *UMP* (95) (10), *UDP* (95) (10), *CDP* (23) (10)	Second phosphorylation step; reversible enzyme
Mt-GMPK*	dGMP, dGDP, *GMP* (17) (26), *GDP* (17) (26)	Second phosphorylation step; reversible enzyme
AK3	dAMP, dADP, *AMP* (139) (74), *ADP* (139) (74)	Second phosphorylation step; reversible enzyme
Nm23-H4, Nm23-H6†, DR-nm23†	dNDP, dNTP, *NDP* (75) (41), *NTP* (75) (41)	NDPK; third phosphorylation step; reversible enzyme
Nucleoside transporter	dA, dT, dC	Transports dN between mitochondria and cytoplasm
Deoxyguanosine transporter	dG	Transports dG between mitochondria and cytoplasm
Deoxynucleotide carrier	dNDP, dNTP	Exchanges di- and triphosphates across the mitochondrial inner membrane
Polymerase-γ	dNTP	Synthesizes mitochondrial DNA

Where numerical values are not given, the K_m values for that enzyme and substrate from Table 2 are used. The underlined inhibitors are not also substrates of the enzyme. Italics indicate ribonucleotide substrates and inhibitors that are held constant in our model. *Gene has not yet been identified at the time of publication. †Although these isoforms have been localized to mitochondria, it is uncertain that they possess activity in the matrix space. TK2, thymidine kinase 2; dGK, deoxyguanosine kinase; dNT-2, deoxynucleotide triphosphate-2; 5′-NT, 5′-nucleotidase; Mt-TMPK, mitochondrial deoxythymidine monophosphate kinase; Mt-UMP-CMP, mitochondrial uridine monophosphate-cytidine monophosphate; Mt-GMPK, mitochondrial guanosine monophosphate kinase; AK3, adenylate kinase 3; NDPK, nucleoside diphosphate kinase.

model of replication, a polymerase starts from O_H and replicates two-thirds of the DNA molecule and then a separate polymerase begins DNA synthesis of the light strand in the reverse direction. Replication is coupled to mtDNA transcription because an RNA primer from transcription is used near O_H for replication initiation.

A different model of synchronous mtDNA replication was recently suggested on the basis of observations of replication intermediates in two-dimensional gels (4). However, extensive verification of this model has yet to be performed, and the model is still controversial. In the simulation, we have used the asynchronous Clayton-Vinograd model.

MtDNA diseases. A number of mitochondrial diseases are caused by errors in the mitochondrial nucleotide metabolism due to nuclear DNA mutations. These diseases include mitochondrial neurogastrointestinal encephalomyopathy (MNGIE), adult dominant and adult recessive progressive external ophthalmoplegia (adPEO and arPEO), Amish microcephaly, and mtDNA depletion syndrome (14, 48). MtDNA mutations and depletion can be caused either by a dysfunction of the mtDNA replicative machinery or by imbalances or deficiencies in the mitochondrial dNTP pools. MtDNA depletion diseases are an extreme form of mitochondrial disease in which the mtDNA in certain cell types is present in very low amounts. Mutations in TK2 and dGK have been shown to cause severe mtDNA depletion (14). Mutations in the mitochondrial adenine nucleotide translocase (ANT), a mtDNA helicase called twinkle, and polymerase-γ cause adPEO (48). Mutations in the cytoplasmic thymidine phosphorylase cause MNGIE, and mutations in the DNC cause Amish microcephaly (66).

Understanding the basic metabolism of deoxynucleotides within mitochondria is a necessary first step in understanding this significant group of mitochondrial diseases. For this reason, we have built a simulation model of this metabolism.

METHODS

Nucleoside transporter and deoxynucleotide carrier models. An ENT in the inner membrane of the mitochondrion allows nucleosides to move between the mitochondrial matrix and the intermembrane space (which we assume to be in equilibrium with the cytoplasm). We used standard Michaelis-Menten kinetics (K_m) to model the nucleoside transport between the mitochondrial matrix and the cytoplasm as follows:

$$R_{\text{transporter},j} = \frac{V_{\max,j}[dN]_{\text{cyto},j}}{K_{\text{m},j}\left(1+\sum_i \frac{[C_i]}{K_{I,i}}\right)+[dN]_{\text{cyto},j}} - \frac{V_{\max,j}[dN]_{\text{matrix},j}}{K_{\text{m},j}\left(1+\sum_i \frac{[C_i]}{K_{I,i}}\right)+[dN]_{\text{matrix},j}} \quad (1)$$

where the subscript j refers to the four nucleoside species, dA, dC, dG, and dT, and i is summed over the competitive inhibitor concentrations ($[C_i]$). We modeled deoxyguanosine (dG) as being transported through a nucleoside transporter separate from the other three deoxynucleosides on the basis of previous experiments (83) (see Table 1). V_{max} and K_m values are the same in both directions and are shown in Tables 2 and 3. Experimental kinetic values for mitochondrial dA, dC, and dT transport are unknown. Therefore, we used values from experiments in which mitochondrial adenosine transport was measured (33).

The DNC exchanges nucleotide diphosphates and triphosphates across the mitochondrial inner membrane. It is not known whether the membrane potential has as strong an effect on the DNC as it does on the related ANT. This effect would preferentially remove dNTPs, which are needed for mtDNA synthesis, from the matrix. Because the influence of the membrane potential on the DNC is not currently known, we have modeled the nucleotide carrier diphosphate/triphosphate exchange as electroneutral, not favoring either dNDP or dNTP exchange into the matrix. For example, electroneutral exchange could occur if triphosphate transport were coupled to a K^+ ion. We used

Table 2. *Micromolar K_m values for the reactions modeled*

dN	Nucleoside Transport	Nucleoside Kinase	Nucleotidase	NMPK	NDPK	dNDP Transporter	dNTP Transporter	Polymerase-γ
A	2	467	1,520	139	75	14	106	0.8
G	0.64	4	560	17	75	55	230	0.8
C	2	11	1,900	17	300	99	423	0.9
T	2	16 ($h = 0.5$)	200	4.9	300	117	595	0.6

The nucleoside kinase reaction for T has negatively cooperative Hill kinetics, with h denoting the Hill coefficient. Nucleoside transport data are from Refs. 33 and 83; nucleoside kinase data are from Refs. 54, 81, and 82; nucleotidase data are from Refs. 24, 51, and 61; NMPK data are from Refs. 10, 19, 26, 55, 73, and 74; NDPK data are from Refs. 16, 38, 41, 53, and 77; dNDP and dNTP transport data are from Ref. 13; and polymerase-γ data are from Refs. 34, 35, 43, and 44. Micromolar K_m values were converted to units of molecules/mitochondrion for the simulation.

standard K_m kinetics to calculate the electroneutral exchange, so the equation has the same form as *Eq. 1*, with dNDP and dNTP concentrations ([dNDP] and [dNTP], respectively) used as substrates. On the basis of previous experiments (13), we assumed that the deoxynucleotide carrier can exchange deoxyribonucleotides for ribonucleotides. Therefore, this carrier can act as a net source or sink of deoxyribonucleotides only when deoxyribonucleotides are exchanged for ribonucleotides. Ribonucleotides are included in the simulation only as competitive inhibitors of this and a few other reactions (Table 1).

Phosphorylation model: K_m dynamics with inhibitions. For all but one (TK2 acting on dT) of the phosphorylation reactions, we calculated the reaction rates using the standard K_m equation, including inhibition from all substrates that also interact with each enzyme. For the reversible reactions, this included the products as inhibitors (see Fig. 2 and Table 1). In general, the reaction rate R_s for a substrate with concentration $[S]$ is calculated as follows:

$$R_S = \frac{V_{max}[S]}{K_m\left(1 + \sum_i \frac{[C_i]}{K_{I,i}}\right) + [S]} \quad (2)$$

The interaction of each substrate $[S]$ with the enzyme is represented by the pair of parameters V_{max} and K_m. Tissue-dependent variations in these reaction rates are caused by differing enzyme levels, modeled by changes in the parameter V_{max}. The forward and reverse V_{max} values for reversible reactions are discussed at the end of METHODS. Parametric values described in the literature are shown in Tables 2 and 3. The sum in the denominator is taken over all $[C_i]$ of this reaction. When the K_i for any competitive inhibitor is not known, the value is taken to be the K_m for that inhibiting chemical.

In experiments using the isolated TK2 enzyme, the nucleoside kinase reaction for dT has been shown to have negatively cooperative Hill kinetics (54). The mathematical model for this is as follows:

$$R_S = \frac{V_{max}[S]^h}{K_m^h\left(1 + \sum_i \frac{[C_i]}{K_{I,i}}\right) + [S]^h} \quad (3)$$

where h is the Hill cooperativity. In this model, the inhibitors do not have cooperative kinetics, based on experimental data for TK2 (54).

MtDNA polymerase model. The mtDNA polymerase requires a special model, which we have developed. The polymerase-γ adds dNTP molecules one at a time to the new strand of mtDNA. Each of the four deoxynucleotides may be added at different rates, denoted by rA, rC, rG, and rT, with each rate depending on the triphosphate concentration of that deoxynucleotide. We used K_m dynamics to model these four rates, with a V_{max} and K_m value for each deoxynucleotide substrate determined on the basis of data reported in the literature (Table 2). Experiments show that polymerase-γ has ~50% the rate of polymerization on double-stranded DNA as it does on the short, overhanging DNA template with which the kinetic values were measured (34, 35, 43), and that adjustment is made to these V_{max} values (Table 3).

Because the deoxynucleotides were added linearly to the growing mtDNA strand, we modeled the total time t to polymerize a segment of mtDNA strand of length L as a linear function as follows:

$$t = \left(\frac{fA}{rA} + \frac{fC}{rC} + \frac{fG}{rG} + \frac{fT}{rT}\right)L \quad (4)$$

where fA, fC, fG, and fT are the fractions of each of the nucleotides to be polymerized into the mtDNA segment. For the heavy strand of mtDNA, these values are 0.247, 0.131, 0.313, and 0.309, respectively. On the basis of these values, using algebra, we can define a total polymerization rate R_{poly} as follows:

$$R_{poly} = \frac{L}{t} = \frac{rA \times rC \times rG \times rT}{fA \times rC \times rG \times rT + fC \times rA \times rG \times rT + fG \times rA \times rC \times rT + fT \times rA \times rC \times rG} \quad (5)$$

Table 3. *Maximum reaction rate values for the model reactions*

	V_{max}, μM·min^{-1}·mg of protein^{-1}							
dN	Nucleoside transport	Nucleoside kinase	Nucleotidase	NMPK	NDPK	dNDP exchange	dNTP exchange	Polymerase-γ, nucleotides/s
G	0.16	0.043	3,000	131	325	0.85	0.85	18.5
A	0.8	0.429	3,000	1,320	325	0.85	0.85	22.5
C	0.8	0.789	3,000	23	140	0.85	0.85	21.5
T	0.8	1.288	74	44	140	0.85	0.85	12.5

References are the same as in Table 2. These V_{max} values were multiplied by the enzyme's molecular mass in kilodaltons and the number of enzymes per mitochondrion (Table 4) to yield the units of molecules/mitochondrion/min used in the simulation.

This is the rate at which the polymerase-γ replicates a strand of mtDNA defined by the parameters fA, fC, fG, and fT. Replication of the mtDNA molecule is modeled as the asynchronous polymerization of the two strands (6). In this model, we used constant values of fA, fC, fG, and fT for each strand, although variation in these values by position along the strand also could be included. The rate of mtDNA synthesis was set at 0 until the replication start time, when we discontinuously set it to R_{poly} to represent the replication of the heavy strand. The amount of new mtDNA polymerized on each strand was calculated, and replication of each strand was stopped, when the length of the newly polymerized mtDNA strand equaled the human mtDNA genome length of 16,568 bp.

Differential equations for the deoxynucleotide concentrations. The individual K_m, Hill, and polymerization equations were used in differential equations for the concentrations of the 16 metabolite pools in our model: *dN*, *dNMP*, *dNDP*, and *dNTP* for each A, C, T, and G. In this section, for clarity, we use only the generic forms of the differential equations. The specific equations for the four phosporylated forms of thymidine are provided as examples in the APPENDIX. The rates of change of the four dN pools are as follows:

$$\frac{d[dN_j]}{dt} = NucsideIn_j - NucsideOut_j - NucKin_j + NucTidase_j \quad (6)$$

where *NucsideIn* is the rate of deoxynucleoside transport into the matrix space, and *NucsideOut* is the rate of deoxynucleoside transport out. *NucKin* is the rate of the nucleoside kinase (TK2 or dGK) reaction, and *NucTidase* is the rate of the nucleotidase reaction.

The rates at which the four dNMP pools change over time are calculated as follows:

$$\frac{d[dNMP_j]}{dt} = NucKin_j - NucTidase_j + NMPKrev_j - NMPKfwd_j \quad (7)$$

where *NMPKfwd* and *NMPKrev* are the rates of formation of *dNDP* and *dNMP* by the forward and reverse reactions of nucleoside monophosphate kinase enzymes.

The rates of change of the four dNDP pools are calculated as follows:

$$\frac{d[dNDP_j]}{dt} = NMPKfwd_j - NMPKrev_j + NDPKrev_j - NDPKfwd_j + DNCdNDPin_j - DNCdNDPout_j \quad (8)$$

where *NDPKfwd* and *NDPKrev* are the rates of formation of dNTP and dNDP by the forward and reverse reactions of the nucleoside diphosphate kinase enzyme. *DNCdNDPin* and *DNCdNDPout* are the rates of dNDP transport into and out of the matrix space by the DNC.

Finally, the rates of change of the four dNTP pools are calculated as follows:

$$\frac{d[dNTP_j]}{dt} = NDPKfwd_j - NDPKrev_j + DNCdNTPin_j - DNCdNTPout_j - (R_{poly} \times fN_j) \quad (9)$$

where *DNCdNTPin* and *DNCdNTPout* are the rates of DNC transport of dNTPs into and out of the matrix space. fN_j is the fraction of A, C, T, or G on a particular strand of mtDNA. R_{poly} is set at 0 when no mtDNA replication event is occurring.

Numerical solution of the differential equations and metabolic control analysis. The simulations were written in Mathematica version 5 software using the numerical differential equation solver for a system of differential and algebraic equations. The Mathematica code and the deoxynucleotide model constants that we used are available online as supplemental material.[1] The solver uses an adaptively selected step size and switches automatically between the Adams predictor-corrector method for nonstiff and backward difference formulas (Gear method) for stiff differential equations.

We used the Metabolic Control Analysis package, which is publicly available for the Mathematica system (46). We used flux response coefficients (36) to measure the extent of the control of the parameters of each enzyme in the system on the polymerization rate in the state with two polymerases active. In this paper, we present data only for the control of the 13 enzyme concentrations (Table 1) on the polymerization rate, because enzyme concentration is the parameter that is the most realistic to vary. We had to take into account the complication that each enzyme takes part in multiple pathways (Fig. 2), so an enzyme concentration had to be varied in the same way in each pathway in which it was involved. In the K_m model, the V_{max} parameters are proportional to the enzyme concentration. So, for the metabolic control analysis, we multiplied all the V_{max} parameters of each enzyme by a normalized enzyme concentration ([enzyme]), set to 1, and measured the change in the polymerization rate due to variations in the 13 [enzyme] terms.

Simulating labeled and unlabeled mtDNA precursors. We have extended the basic model to represent labeled and unlabeled deoxynucleotides, equivalent to radioactive or fluorescent labeling in the laboratory. Separate differential equations were set up for the labeled and unlabeled forms, with the reaction rates determined using the total concentration of labeled plus unlabeled deoxynucleotides. Each of the dN pool equations (*Eqs. 6–9*) was replaced by a pair of differential equations, with one representing the labeled form and one representing the unlabeled form. For example, for the deoxynucleoside pools (*Eq. 6*), we have the following two sets of equations. For the labeled deoxynucleosides, represented by a prime on the concentrations, we have

$$\frac{d[dN_j]'}{dt} = NucsideIn_j\left(\frac{[dN_j]'_{cyto}}{[dN_j]_{cyto} + [dN_j]'_{cyto}}\right) - (NucsideOut_j + NucKin_j)\left(\frac{[dN_j]'}{[dN_j] + [dN_j]'}\right) + NucTidase_j\left(\frac{[dNMP_j]'}{[dNMP_j] + [dNMP_j]'}\right) \quad (10)$$

For the corresponding unlabeled deoxynucleoside, we have

$$\frac{d[dN_j]}{dt} = NucsideIn_j\left(\frac{[dN_j]_{cyto}}{[dN_j]_{cyto} + [dN_j]'_{cyto}}\right) - (NucsideOut_j + NucKin_j)\left(\frac{[dN_j]}{[dN_j] + [dN_j]'}\right) + NucTidase_j\left(\frac{[dNMP_j]}{[dNMP_j] + [dNMP_j]'}\right) \quad (11)$$

Note that adding *Eqs. 10* and *11* restores the original *Eq. 6*.

This method also can be used to trace the flow of material through the mitochondrion. By starting the simulation with no deoxynucleotides or deoxynucleosides in the mitochondrion, with all of the cytoplasmic deoxynucleosides labeled and all of the cytoplasmic deoxynucleotides unlabeled, we measured the amount of dNTP incorporated into DNA from the cytoplasmic deoxynucleoside pools (through the nucleoside transporter route) and compared it with that originating in the cytoplasmic deoxynucleotide pools.

Defining simulated cell types. We defined three categories of normal cells: rapidly dividing cells, slowly dividing cells, and postmitotic cells. To this list we add a fourth abnormal cell type: cancer

[1] Supplementary material for this article is available directly from the authors and also can be found at http://ajpcell.physiology.org/cgi/content/full/00530.2004/dc1.

Table 4. *Enzyme levels and molecular mass*

	ENT G	ENT A, T, and C	dGK	TK2	5′-NT	dNT2	AK3	TMPK	GMPK	CMPK	NDPK	DNC
Enzyme level, molecules/mitochondrion	38*	38	200	100	50*	50	450	50*	50*	50*	300	500
Molecular mass, kDa	50	50	28	28	25	25	26	24	25	25	66	32

Values were calculated as described in METHODS. *No reference for expression available. Levels of similar mitochondrial enzymes were used when no data were available. ENT, equilibrative nucleoside transporter; DNC, deoxynucleotide carrier.

cells. Cancer cells are of interest in this model because the normal cytoplasmic nucleotide metabolism is altered in these cells and because cancer cells often show mtDNA mutations that might be caused by this altered metabolism. In principle, the enzyme concentrations in the model could be different in every cell type. However, the limited expression data available do not indicate that the enzyme levels of this metabolism vary greatly across cell types (18). For a simple model, we kept the enzyme levels constant across these four cell type categories (Table 4) and distinguished the cell categories by the cytoplasmic deoxynucleotide diphosphate and triphosphate concentrations (Table 5).

Many cytoplasmic enzymes involved in cytoplasmic dNTP synthesis are cell cycle regulated, because >99% of cellular dNTPs are used during the S phase of the cell cycle while nuclear DNA is replicating. These regulated enzymes include ribonucleotide reductase, thymidylate synthase, TK1, and thymidylate kinase (64). In slowly dividing and postmitotic cells, cytoplasmic deoxynucleotide levels are substantially less than in rapidly dividing cells, owing to the downregulation of these enzymes (7, 80). Data from nondividing compared with dividing HepG2 liver cells, as well as from resting compared with stimulated lymphocytes, show an ~10-fold increase in cytoplasmic dNTP levels in dividing cells over resting cells (20, 21, 32). On the basis of this and other data, we set cytoplasmic deoxynucleotide levels to simulate the four classes of cell type: cancerous, rapidly dividing, slowly dividing, and postmitotic cells (Table 4) (20, 21, 76). The cytoplasmic deoxynucleoside concentrations were kept at a constant level (12, 27, 59, 69) because it is not known whether they also vary with the cell cycle, although it is likely that cell cycle regulation does occur in some cell types (57, 79).

Determining enzyme levels in the mitochondrion. For this simulation, the units of reaction rate and of the V_{max} parameters are molecules per mitochondrion per minute. The standard units reported in the literature are micromoles per milligram of enzyme per minute, so we must use the number of enzyme molecules per mitochondrion and the enzyme molecular weight (Table 4) to convert data to the units needed in the simulation. Enzyme levels are measured by three basic methods; inhibitor binding, enzyme activity measures, and blotting experiments. Each method requires a different conversion.

The ENT levels were calculated from ligand binding experiments (5, 33, 58). An inhibitor of nucleoside transport was found to have 2,100 fmol/mg of mitochondrial protein binding sites. We used 3.3×10^{10} mitochondria/mg of mitochondrial protein, a value averaged from the values reported in the literature [ranging from 4.3×10^{9} (22) to 5.3×10^{10} (56)] to convert this value to transporters per mitochondrion.

TK2, dGK, AK3, and dNT-2 enzyme levels were calculated from enzyme activity measurements (1, 17, 55, 63, 75). In these experiments, saturating substrate concentrations were administered to a known mass of mitochondria, so the number of molecules of enzyme present may be calculated using the known V_{max} of the enzyme. For TK2 and dGK, an average value from several tissues was used.

DNC levels were approximated from Western blotting experiments (13) by comparison to a known quantity of recombinant DNC that was used as a standard. NDPK levels were roughly estimated from blotting experiments (39, 52, 53). These experiments showed that NDPK was highly expressed, so the number of enzymes per mitochondrion was set at 300, a relatively high value compared with the other levels shown in Table 4.

Unknowns in the model. In the mitochondrial matrix, adenylate kinase (AK3) phosphorylates dAMP (55, 74). It is hypothesized that a dCMP kinase phosphorylates dCMP and that a guanylate kinase phosphorylates dGMP in mammalian mitochondria, but such proteins have not yet been identified (10, 84). None of the kinetic values in the model were functionally determined (i.e., with values set to produce a particular behavior in the simulation). When values were not available, the values from the corresponding cytoplasmic enzymes were used.

It was reported previously that cells had only one type of dTMP kinase activity that is located in both the cytoplasm and the mitochondrion (42). However, this initial observation has yet to be confirmed.

Table 5. *Cytoplasmic nucleotide and nucleoside concentrations used*

	Mean, μM (range)			
	Cancer cells	Rapidly dividing cells	Slowly dividing cells	Postmitotic cells
Nucleosides				
dA, dC, dG, dT	0.5	0.5	0.5	0.5
Diphosphates				
dADP	5 (2–8)	2 (0.6–4)	0.7 (0.1–1.3)	0.07 (0.01–0.13)
dCDP	4 (2.8–5.6)	2 (0.8–3.6)	1.0 (0.1–2.9)	0.10 (0.01–0.29)
dGDP	4 (0.6–8)	1 (0.2–1.6)	0.8 (0.1–1.6)	0.08 (0.01–0.16)
dTDP	6 (3.6–11)	4 (1.6–7.6)	2.5 (0.1–5.6)	0.25 (0.01–0.56)
Triphosphates				
dATP	25 (10–40)	10 (3–20)	0.7 (0.1–1.3)	0.7 (0.1–0.13)
dCTP	20 (14–28)	10 (4–18)	1.0 (0.1–2.9)	0.10 (0.01–0.29)
dGTP	20 (3–40)	5 (1–8)	0.8 (0.1–1.6)	0.08 (0.01–0.16)
dTTP	30 (18–55)	20 (8–38)	2.5 (0.1–5.6)	0.25 (0.01–0.56)

Cytoplasmic monophosphate levels are not needed, because they are not transported into the mitochondrion. Nucleoside levels are from Refs. 12, 69, and 76 and are assumed to be constant throughout the cell types. Triphosphate levels in cancer cells are from Refs. 30, 50, 67, and 76. Triphosphate levels for rapidly dividing cells are from Refs. 8, 12, 20, 21, 49, 70–72, and 76. Triphosphate levels in slowly dividing cells are from Refs. 7, 21, 28, 47, 50, 67, and 71. Triphosphate levels in postmitotic cells were set 10-fold lower than in slowly dividing cells. Diphosphate levels were set to 20% of the triphosphate levels in cancer and rapidly dividing cells in accordance with the ADP-to-ATP ratio and equal to dNTP concentrations in slowly dividing and postmitotic cells, because there have been some reports of cytoplasmic diphosphate levels higher than triphosphate levels in these cell types (50).

Mitochondria have been shown to possess a general nucleotidase that dephosphorylates nucleotide monophosphates (61). Whether the activity resides in the matrix space, however, remains controversial.

The relative forward and reverse reaction rates for mitochondrial nucleoside monophosphate kinases and NDPK are not known. However, the concentrations of mitochondrial dTMP, dTDP, and dTTP have been shown in experiments to be in the same proportions as concentrations of mitochondrial AMP, ADP, and ATP (60). In our model, mitochondrial AMP, ADP, and ATP concentrations are set at 8.0, 6.0, and 2.9 mM (76). We assume that the proportions of dTMP, dTDP, and dTTP are determined primarily by the rates of the forward and reverse phosphorylation reactions. We used these experimental results to set the maximum velocity of the reverse NDPK reaction to 75% (6.0/8.0) of the forward reaction, based on the ADP-to-ATP ratio. We also set the maximum velocities of the reverse NMPK reactions to ~50% (~2.9/6.0) of the forward reactions using the AMP-to-ADP ratio.

RESULTS

Mitochondrial deoxynucleotide levels. In Fig. 3, we show the mitochondrial dN, dNMP, dNDP, and dNTP levels from simulations of cancerous, rapidly dividing, slowly dividing, and postmitotic cells. The simulation begins in a steady state, with no mtDNA polymerases active. In steady state, the dNMP, dNDP, and dNTP concentrations are roughly proportional to the ribonucleotide AMP, ADP, and ATP concentrations in the dividing cell simulations; but in postmitotic cell simulations, the relative proportions of dNMP, dNDP, and dNTP in the mitochondrion vary depending on the specific nucleotide (Fig. 3). In cancer and rapidly dividing cells, the steady-state dNTP levels in the simulated mitochondrion are approximately one-half the cytoplasmic levels (Table 5 and Fig. 3). However, in slowly dividing and postmitotic cells, the mitochondrial dNTP levels rise slightly above or are nearly equal to those in the cytoplasm.

At 60 min in the cancerous and rapidly dividing cell's mitochondrion (150 and 600 min in the slowly dividing and postmitotic cell's mitochondrion), we began the replication of a single mtDNA molecule as described in METHODS. The existing nucleotide pools in the mitochondrion were quickly drained, and the mtDNA replication must rely on material imported from the cytoplasm for the majority of the mtDNA precursors. As the replication of each strand begins or ends, the deoxynucleotide concentrations rapidly shift to new equilibrium values at which the rate of dNTP incorporation into the mtDNA equals the rate of nucleotide and nucleoside entry into the mitochondrion. Because the heavy and light strands have different base compositions, the steady-state mitochondrial dNTP concentration levels differ during the replication of the different strands. The three phases of replication in this model are shown in Fig. 3. The large changes in dNTP levels during the mtDNA replication cause very large changes in the ratios of the four deoxynucleotides (Fig. 3, *Q–T*). These changes are most extreme for the slowly dividing and postmitotic cells, in which the dTTP-to-dCTP ratio exceeds 30 at some points in the replication. Imbalances of this size or even smaller have been shown to increase the chance of mtDNA mutation (72).

Different cell types have markedly different cytoplasmic deoxynucleotide levels. Because the cytoplasmic and mitochondrial deoxynucleotide pools are coupled, we would expect the cytoplasmic deoxynucleotide levels to have a strong effect on mtDNA replication time (Fig. 4). The minimum replication

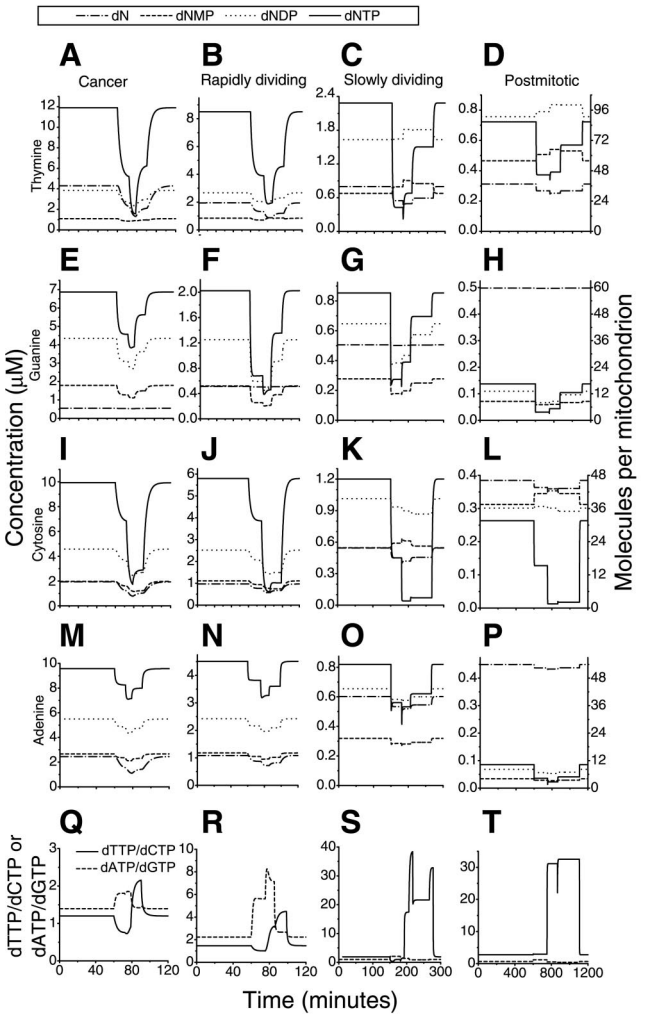

Fig. 3. Deoxynucleoside and deoxynucleotide levels in mitochondria. *A–T*: deoxynucleotide type (thymine, guanine, cytosine, or adenine), except the *bottom row*, which indicates the dTTP-to-dCTP or dATP-to-dGTP ratio. Columns indicate cell type (cancer, rapidly dividing, slowly dividing, or postmitotic). One micromole equals 120 molecules per mitochondrion.

time in the simulation is ~30 min and occurs when the mitochondrial dNTP concentrations are high enough to saturate the polymerase-γ reaction rate. The replication time of ~40 min in our simulated dividing cells is slightly faster than the time of ~60 min found experimentally (6).

At the left side of Fig. 4, the very long replication times at low cytoplasmic deoxynucleotide levels are due to the very slow phosphorylation of dA by dGK. This forces the mtDNA replication to rely on the low cytoplasmic dATP pool for mtDNA replication, because the phosphorylation of dA within the mitochondrion is so slow. One advantage of a simulation is that thought experiments can be performed, and we show one such experiment in the inset in Fig. 4. What if the activity of dGK on dA were higher than the reported K_m and V_{max}? The inset shows that we raised the reaction rate of dGK on dA to that of TK2 on deoxythymidine, the fastest of the mitochondrial nucleoside phosphorylations. In this case, the replication time plateaus at a maximum of ~800 min in postmitotic cells. The plateau occurs because the mitochondria are then dependent almost solely on deoxynucleoside import and are thus insensitive to the cytoplasmic deoxynucleotide levels.

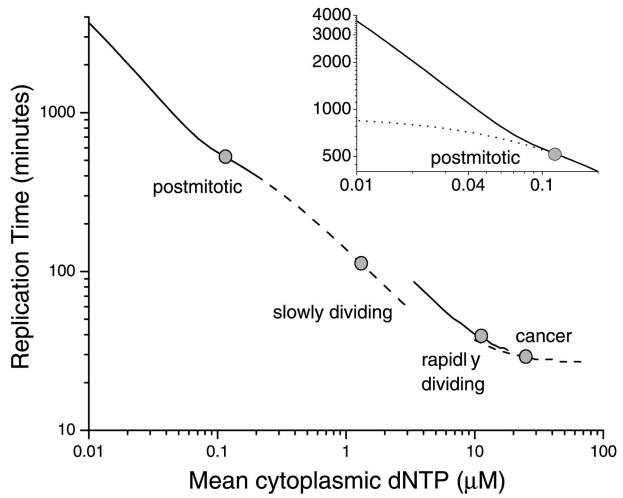

Fig. 4. Replication times in different cell types. The time taken to copy one simulated mtDNA molecule was measured at different cytoplasmic dNTP concentrations. The cytoplasmic deoxynucleotide concentrations were varied proportionately throughout the range shown for each cell type using the definitions in Table 5. Circles mark the standard values representing the cell type shown. Dotted line in *inset* shows the effect of increasing the reaction rate for the phosphorylation of dA.

On the basis of electron microscopic studies of mtDNA replication intermediates, Robberson et al. (65) hypothesized that the replication rate was nearly linear along the circular mtDNA molecule because all intermediates were observed in nearly equal amounts. For comparison with their observation, we calculated the polymerization rates of both the heavy and light strands in our simulation as a function of the position on the mtDNA molecule in different cell types (Fig. 5). High initial polymerization rates dropped quickly as the nucleotide levels dropped in the matrix. The rate of heavy-strand polymerization also decreased when light strand polymerization was initiated and both polymerases were operating simultaneously. Later, the light strand polymerization rate increased when the heavy strand synthesis completed. Despite these relatively minor changes, mtDNA polymerization rates in this simulation are fairly uniform across the mtDNA molecule.

Nucleotide flow through the mitochondrion and into mtDNA. We were able to define only three routes of material net flow through the mitochondrion (Fig. 6), because *1*) there are transporters for both deoxynucleosides and deoxynucleotides in mitochondria, *2*) all of the phosphorylation steps are reversible, and *3*) there are no sources of deoxynucleotides within the mitochondrion. A phosphorylating state occurs if the net flow through the nucleoside transporter is inward to the mitochondrion while that through the DNC is outward to the cytoplasm. A dephosphorylating state occurs when the net flow through the DNC is inward and that through the nucleoside transporter is outward. This state requires a matrix space nucleotidase, which may not be expressed in all cell types (61). Last, an efficient state occurs if flow through both transporters is inward. The efficient state can occur only as a steady state during mtDNA replication, when the material flowing inward through both the DNC and the nucleoside transporter ends up in the replicating mtDNA. Because there is no source of nucleotides within the mitochondrion, the state with a net outward flow from both the DNC and the nucleoside transporter is not possible as a steady state.

The net fluxes through either the nucleoside transporter and the DNC over the time course of replication of one mtDNA molecule are shown in Fig. 7. During the steady state (when no mtDNA replication is occurring) in cancer cells and in rapidly or slowly dividing cells, the mitochondria are in the dephosphorylating state, with positive flux through the DNC and an equal but negative flux through the nucleoside transporter. In postmitotic cells, steady-state flow reverses and the phosphorylating state occurs. During replication, net fluxes into the matrix space increase through each route. However, the DNC flux increases to a greater extent during replication in all cell types. In postmitotic cells, the DNC flux increase is just slightly greater than that of the nucleoside transporter.

Figure 8 shows the net flux of deoxynucleosides and deoxynucleotides through mitochondria averaged over the replication time of one molecule of mtDNA. All four deoxynucleotides show the same pattern. At low cytoplasmic dNTP concentrations, the mitochondrion is in the phosphorylating state. At high cytoplasmic dNTP concentrations, the organelle is in the dephosphorylating state, and between the two is a short concentration range that is in the efficient state. The

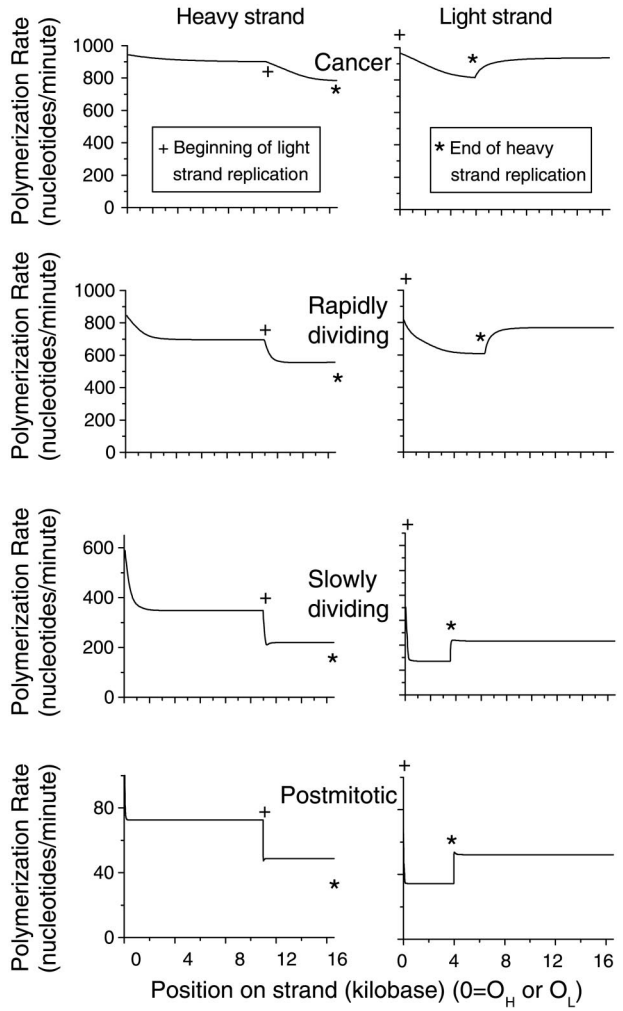

Fig. 5. Heavy and light strand polymerization rates. The polymerization rates of each strand were plotted against the distance in bp away from the origin of replication for that strand. O_H, origin of replication for heavy strand of mtDNA; O_L, origin of replication for light strand of mtDNA.

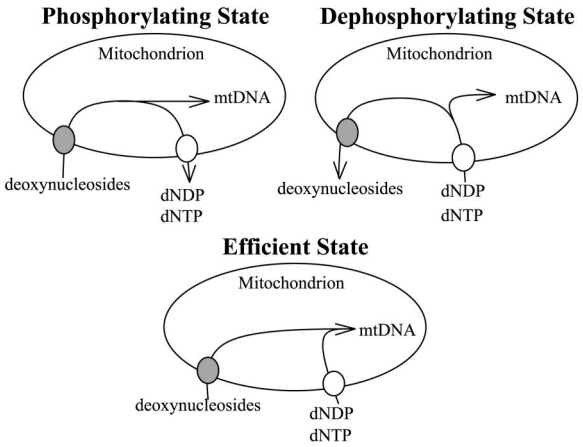

Fig. 6. Schematics showing possible routes of net nucleotide flux through mitochondria.

fluxes in the steady state (i.e., when no mtDNA replication is occurring) show the same pattern as that shown in Fig. 8 (data not shown) with regard to the loss of the efficient state, which can occur only during mtDNA polymerization. For dA, the phosphorylating state occurs only at an unreasonably low cytoplasmic dATP concentration, so it always has a positive net transport rate into the matrix space by the DNC in our model.

Percentage of mtDNA precursors transported by the nucleoside transporter or DNC. Because the number of deoxynucleotide molecules within the mitochondrial matrix is far too small to support a full replication of even a single mtDNA molecule (15), the majority of the mtDNA precursors are imported into the mitochondrion from the cytosol during the mtDNA replication process. These precursors may be imported through the nucleoside transporter or by the DNC. Using the simulation of labeled deoxynucleotides and deoxynucleosides, we can calculate the source of each dNTP that is incorporated into the replicating mtDNA molecule. We begin this simulation with no deoxynucleosides or deoxynucleotides within the mitochondrion, allow the mitochondrial deoxynucleotide pools to come to a steady state (recording the source of the deoxynucleotides, DNC, or nucleoside transporter), and then simulate an mtDNA replication (still recording the source of the mtDNA precursors). In rapidly and slowly dividing cells, the vast majority of deoxynucleotides in mtDNA are phosphorylated in the cytoplasm and transported into the mitochondrion by the DNC (Fig. 9). In postmitotic cell simulations, about one-half the deoxynucleotides in mtDNA are imported into mitochondria as deoxynucleosides, phosphorylated locally, and then incorporated into DNA. Note that this finding is not in conflict with Figs. 7 and 8, which show postmitotic cells with a net export of material through the DNC. Even though the net flow of deoxynucleotides is outward through the DNC in these cells, there is still some inward flow of deoxynucleotides that end up in the newly synthesized mtDNA.

In all simulated cell types, dA nucleotides are almost exclusively (>96%) imported from the cytoplasm into the matrix space by the DNC. The reason for this is the very slow kinetics of the phosphorylation of dA by dGK in the mitochondrion. Of the four deoxynucleosides, dT is the most efficiently phosphorylated in the mitochondrion, owing to the rapid kinetics of dT with TK2.

Metabolic control analysis. One of the most important uses of metabolic modeling is determining the enzymes that exert the most control over the system. To obtain this information, metabolic control analysis (MCA) may be performed on the steady states of the system. MCA also indicates the sensitivity of the system to changes in parameter values. The Clayton-Vinograd model of mtDNA replication has four steady states: no polymerization, polymerization of just the heavy strand of mtDNA, polymerization of both strands, and polymerization of just the light strand of mtDNA. In the example shown here, we chose to perform MCA at the steady state when both the heavy

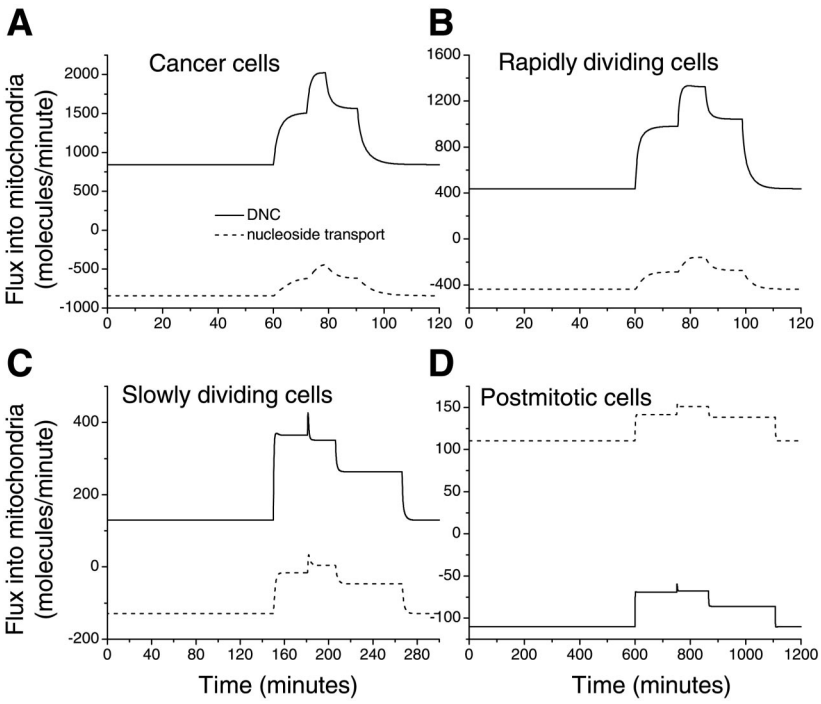

Fig. 7. Net deoxynucleotide carrier (DNC) and nucleoside transporter flux through the replication of one mtDNA molecule. A polymerization event was initiated at 60 min in cancer cells (*A*) and rapidly dividing cells (*B*), at 150 min in slowly dividing cells (*C*), and at 600 min in postmitotic cells (*D*).

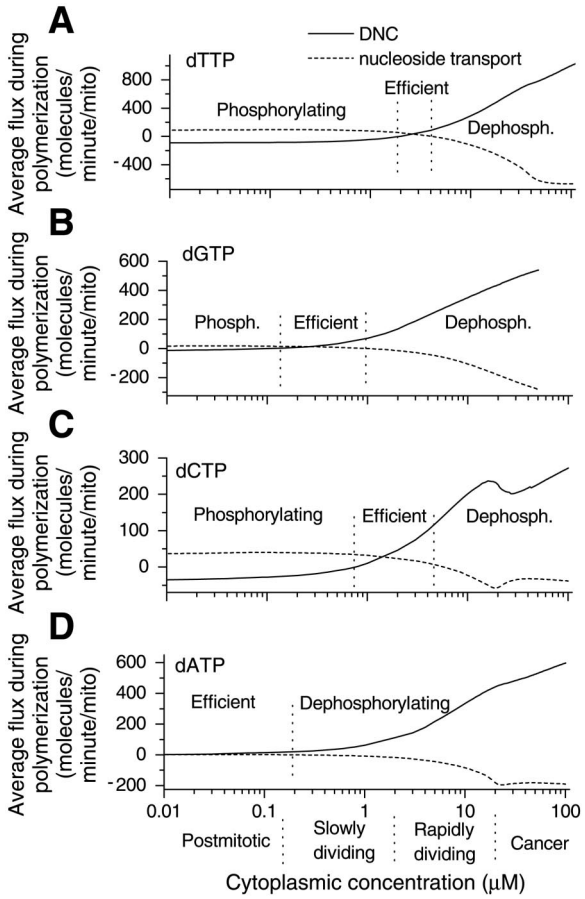

Fig. 8. Net flux during polymerization through the DNC and nucleoside transporter in different cell types (*A–D*). To make the pattern in the phosphorylation series clear, a ratio of 4:2:2:1 for cytoplasmic dTTP:dATP:dCTP:dGTP was maintained in all simulations. The dNDP concentrations were set to dNTP/2.5.

and light strands were replicating. Under this condition, dCTP has the lowest concentration of the four dNTPs and appears to have limited polymerization in all cell types examined (Fig. 3). In Fig. 10, we show the enzymes with a flux-response coefficient of the polymerization reaction of magnitude >0.1 in any of the four simulated cell types.

From our control analysis, the nucleoside transporter does not have much control in dividing cells, but this control increases in postmitotic cells as the cytoplasmic nucleotide concentrations decrease and mitochondria rely more on this route of transport. TK2 follows a similar trend, but with more control than nucleoside transport. 5′-NT exerts negative control on the polymerization rate in postmitotic cells because it opposes the TK2 reaction, which is so important under these conditions. NDPK increases control as cytoplasmic deoxynucleotides decrease. This occurs because cytoplasmically imported dNTPs that bypass this reaction are not plentiful in slowly dividing and postmitotic cells. The DNC is very controlling in rapidly dividing cells, as we expected on the basis of the results for the primary routes of material transport in the different cell types (Fig. 8), and shares the most control with NDPK in slowly dividing cells. The flux-response coefficient is negative in postmitotic cells because the DNC actually slows the polymerization rate in these cells by exporting deoxynucleotides. Finally, we should note that the mitochondrial matrix NDPK enzyme levels are not well known quantitatively, and because this enzyme does have a relatively high control value for mtDNA polymerization in postmitotic cells, this may be a major source of error in our mtDNA replication time in postmitotic cells.

DISCUSSION

Low number of deoxynucleotide molecules in mitochondria. With the dNTP concentrations in the mitochondrion [which are in agreement with cell culture experiments (62)] and the small volume of the mitochondrial matrix of an individual organelle (2×10^{-16} L) (11, 22, 23), the total number of dNTP molecules within an organelle is far too small to support the replication of even a single mtDNA molecule (15). This is true even counting all phosphorylated and nonphosphorylated forms of each deoxynucleotide, not just the dNTPs that are directly used to replicate the DNA. Therefore, the deoxynucleotide pools within the mitochondrion are quickly drained during an mtDNA replication event, and the remaining material must be supplied from the cytoplasm through either the nucleoside transporter or the DNC (Fig. 1). For the simulated postmitotic and slowly dividing cells, the number of deoxynucleotides per organelle can drop to rather low values during a replication event. The use of continuous differential equations to calculate reaction rates provides a good approximation down to ~100 molecules (78). There may be effects in the postmitotic and slowly dividing cells, in which deoxynucleotide numbers per mitochondrion can be very low, that would appear in only a far more complicated, stochastic, and discrete numerical model.

Comparison to experiments with labeled thymidine. Many experiments have been performed administering labeled thymidine to cells in culture that either possessed or were lacking the cytosolic thymidine kinase TK1 (3, 60, 62). In $TK1^-$ cells, the only enzyme that phosphorylates thymidine is the mitochondrial enzyme TK2. Therefore, all labeled thymidine nucleotides in these cells had to be phosphorylated in the mitochondria. Thymidine administered to normal (i.e., $TK1^+$) cells could first be phosphorylated in the cytoplasm and then enter

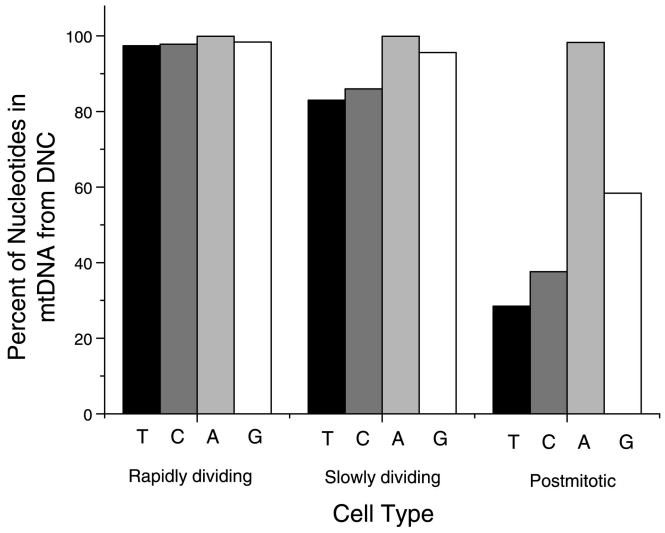

Fig. 9. Percentage of mtDNA nucleotides derived from transport by the DNC in different cell types. Cytoplasmic deoxynucleotide levels were set as shown in Table 5 to represent the different cell types.

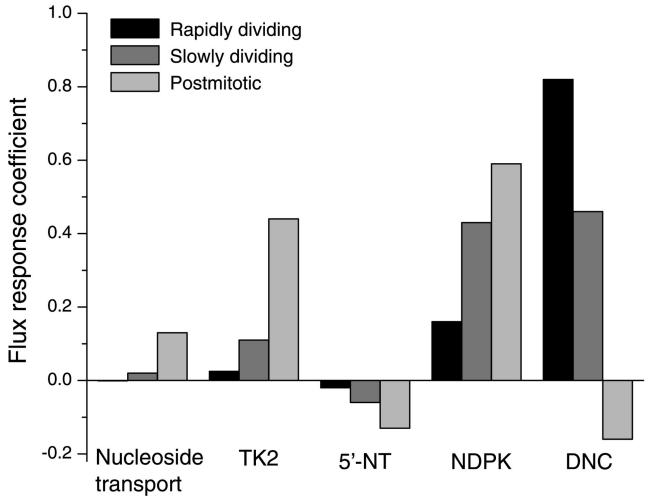

Fig. 10. Flux-response coefficients for polymerization in rapidly dividing, slowly dividing, and postmitotic cells. The steady state with two active polymerases was analyzed. Enzymes not shown had response coefficients <0.1 in all three types of simulated cells.

the mitochondrion through the DNC. Measuring the specific activity, the amount of labeled dTTP compared with total dTTP, or the amount of labeling in mtDNA compared with the amount of total mtDNA in both cell types lets one determine the predominant route of transport in situ. Experiments using $TK1^-$ and $TK1^+$ cultured mouse L cells demonstrated that 95% of thymidine in mtDNA was transported into mtDNA after it had first been phosphorylated in the cytoplasm (3). Experiments measuring cytoplasmic dTTP recently confirmed these observations (60). Therefore, the DNC is almost the sole provider of thymidine under these conditions. Our simulation showed that 98% of the thymidine in mtDNA (Fig. 9) in simulated dividing cells was transported through the DNC, a finding that is in excellent agreement with the value observed in experiments.

Efflux of mitochondrial nucleotides. Our model allows the efflux of nucleotides from the mitochondrion into the cytoplasm through the DNC (Fig. 9). In the early 1970s, Berk and Clayton (3) found almost exclusive labeling of mtDNA (but not nuclear DNA) by administering labeled thymidine to $TK1^-$ cells. The specific activity of nuclear DNA in their experiment was 3% of the mtDNA and <0.05% that of nuclear DNA in $TK1^+$ cells. Therefore, for >25 years, it had been assumed that mitochondria used their nucleotides in mtDNA and did not export them to the cytoplasm. Others have also used $TK1^-$ cells and bromodeoxyuridine to exclusively label mtDNA as well (2, 45). However, recent experiments (62) refuted this conclusion by measuring a strong efflux of labeled dTTP from mitochondria into the cytoplasm. The disagreement between these experiments may be due to differing DNC properties in different cell types (31). The simulations followed the recent experimental data (62) more closely when mitochondrial deoxynucleotide efflux was allowed to occur in the model (i.e., our standard model) than when efflux through the DNC was completely blocked in the simulation (data not shown).

Model significance and suggestions for new studies. On the basis of our simulations of mitochondrial deoxynucleotide metabolism, we draw five main conclusions that could be used as testable hypotheses in future experiments.

1. The deoxynucleotide pools within each mitochondrion are not sufficient to support even a single mtDNA replication (see Fig. 3). Deoxynucleotides and/or deoxynucleosides must be imported into the organelle from the cytoplasm during mtDNA replication. The rate of this import and the concentration of dNTPs in the cytoplasm have a strong effect on the replication time for mtDNA.

2. The mtDNA replication time is quite long in simulations of postmitotic cells in which cytoplasmic deoxynucleotide levels are low (see Fig. 4). The slow reaction rate of dGK for dA is the primary cause of this finding in our model. We suggest that the kinetics of this reaction may be more rapid in vivo than those measured with the purified enzyme. This becomes important when cytoplasmic dADP and dATP concentrations fall below 0.1 μM. This simulation result emphasizes the importance of conducting experiments on postmitotic cells, not just on easily cultured dividing cells, because the behavior of the mtDNA can be significantly different in the two types of cells, and it is the postmitotic cells that are primarily of medical relevance.

3. The deoxynucleotide metabolism within the mitochondrion can be described by three states: phosphorylating, efficient, and dephosphorylating (see Fig. 6). In rapidly dividing cells, the mitochondria act as net sinks for deoxynucleotides and net sources for deoxynucleosides in the cytoplasm. In postmitotic cells, the reverse is true, with mitochondria exporting dNTPs and dNDPs into the cytoplasm.

4. The main controlling enzyme of this metabolism in rapidly dividing cells is the DNC (see Fig. 10). The control parameters are very different in simulated postmitotic cells, with control held mainly by NDPK (the final phosphorylation) and TK2 (the first phosphorylation).

5. Rapidly dividing cells derive almost all of their mtDNA precursors as dNDPs and dNTPs from the cytoplasm (see Fig. 9). Aside from the final phosphorylation of dNDP to dNTP, the nucleotide metabolism in the mitochondrion does little to support mtDNA replication in these cells.

Let us end with a discussion of two of the assumptions of this simulation. In this simple model, we have assumed equal enzyme levels in the four simulated cell types, based on the observation of equal expression levels for most of these enzymes in many tissues (1). It is possible that enzyme levels are varied across cell types by posttranslational modifications or degradation control to put the mitochondria into the efficient state of deoxynucleotide metabolism, or at least closer to it. There is evidence for variable enzyme levels with tissue types of TK2 and dNT-2. The enzyme dNT-2 is highly expressed in postmitotic tissues (heart, brain, and skeletal muscle) (63). Activity of TK-2 was observed to be 10 times lower in skeletal muscle than in liver, fibroblasts, and heart tissue (68). Both of these variations would extend the range of the efficient state of dT metabolism shown in Fig. 8.

Finally, we have assumed a volume of 2×10^{-16} L for the mitochondrion (11, 22, 23). For the purposes of this model, this volume should represent the volume within the mitochondrial matrix from which a replicating mtDNA molecule can take dNTP molecules. The formation of large networks of mitochondria in some cell types could reduce the need to import mtDNA precursors from the cytoplasm during mtDNA replications if the inner membranes of the connected mitochondria also were fused to allow the free movement of dNTPs within the matrix of the network.

Model limitations. The most important limitations of this model are the lack of kinetic data for the nucleoside monophosphate kinases, the possible existence of other deoxynucleotide transporters, the effect of membrane potential on DNC transport, and the unknown concentrations of cytoplasmic dNTPs in postmitotic tissues. We are also concerned with the ability of K_m kinetics to model the system when the enzyme concentrations are nearly equal to the substrate concentrations. This concern holds for all models in which the metabolites are present in submicromolar quantities. Another limitation of the model is the ability of the polymerization equation to reflect polymerase kinetics in postmitotic cells. The kinetics of mitochondrial polymerase-γ were measured under saturating dNTP conditions (34). This is adequate for modeling rapidly dividing cells, but the kinetics may be more complex when the dNTP concentrations are low and not saturating the enzyme. A more detailed model may be necessary to describe polymerization kinetics in this case.

APPENDIX

The differential equations for the mitochondrial thymidine deoxynucleotide pools are listed below as examples. The other three deoxynucleotide pools for each phosphorylated state have similar equations, but with different inhibitors:

$$\frac{d[dT]}{dt} = \frac{V_{max,4,1}[dT]_{cyto}}{K_{m,4,1}\left(1 + \frac{[dA]_{cyto}}{K_{I,1,1}} + \frac{[dC]_{cyto}}{K_{I,3,1}}\right) + [dT]_{cyto}} - \frac{V_{max,4,1}[dT]}{K_{m,4,1}\left(1 + \frac{[dA]}{K_{I,1,1}} + \frac{[dC]}{K_{I,3,1}}\right) + [dT]} - \frac{V_{max,4,2}[dT]^h}{K^h_{m,4,2}\left(1 + \frac{[dTTP]}{K_{I,dTTP}} + \frac{[dCTP]}{K_{I,dCTP}} + \frac{[dC]}{K_{I,dC}}\right) + [dT]^h} + \frac{V_{max,4,3}[dTMP]}{K_{m,4,3} + [dTMP]} \quad (A1)$$

$$\frac{d[dTMP]}{dt} = \frac{V_{max,4,2}[dT]^h}{K^h_{m,4,2}\left(1 + \frac{[dTTP]}{K_{I,dTTP}} + \frac{[dCTP]}{K_{I,dCTP}} + \frac{[dC]}{K_{I,dC}}\right) + [dT]^h} - \frac{V_{max,4,3}[dTMP]}{K_{m,4,3} + [dTMP]} + \frac{0.5V_{max,4,4}[dTDP]}{K_{m,4,4}\left(1 + \frac{[dTMP]}{K_{I,4,4}}\right) + [dTDP]} - \frac{V_{max,4,4}[dTMP]}{K_{m,4,4}\left(1 + \frac{[dTDP]}{K_{I,4,4}}\right) + [dTMP]} \quad (A2)$$

$$\frac{d[dTDP]}{dt} = \frac{V_{max,4,4}[dTMP]}{K_{m,4,4}\left(1 + \frac{[dTDP]}{K_{I,4,4}}\right) + [dTMP]} - \frac{0.5V_{max,4,4}[dTDP]}{K_{m,4,4}\left(1 + \frac{[dTMP]}{K_{I,4,4}}\right) + [dTDP]} + \frac{0.75V_{max,4,5}[dTTP]}{K_{m,4,5}\left(1 + \frac{[dTDP]+[dCDP]+[dCTP]}{K_{I,4,5}} + \frac{[dADP]+[dGDP]+[dATP]+[dGTP]}{K_{I,2,5}} + \frac{[ADP]+[ATP]}{K_{I,NDP}}\right) + [dTTP]} - \frac{V_{max,4,5}[dTDP]}{K_{m,4,5}\left(1 + \frac{[dTTP]+[dCDP]+[dCTP]}{K_{I,4,5}} + \frac{[dADP]+[dGDP]+[dATP]+[dGTP]}{K_{I,2,5}} + \frac{[ADP]+[ATP]}{K_{I,NDP}}\right) + [dTDP]} + \frac{V_{max,4,6}[dTDP]_{cyto}}{K_{m,4,6}\left(1 + \frac{[dCDP]_{cyto}}{K_{I,3,6}} + \frac{[dGDP]_{cyto}}{K_{I,2,6}} + \frac{[dADP]_{cyto}}{K_{I,1,6}} + \frac{[dCTP]_{cyto}}{K_{I,3,7}} + \frac{[dGTP]_{cyto}}{K_{I,2,7}} + \frac{[dATP]_{cyto}}{K_{I,1,7}} + \frac{[dTTP]_{cyto}}{K_{I,4,7}}\right) + [dTDP]_{cyto}} - \frac{V_{max,4,6}[dTDP]}{K_{m,4,6}\left(1 + \frac{[dCDP]}{K_{I,3,6}} + \frac{[dGDP]}{K_{I,2,6}} + \frac{[dADP]}{K_{I,1,6}} + \frac{[dCTP]}{K_{I,3,7}} + \frac{[dGTP]}{K_{I,2,7}} + \frac{[dATP]}{K_{I,1,7}} + \frac{[dTTP]}{K_{I,4,7}}\right) + [dTDP]} \quad (A3)$$

$$\frac{d[dTTP]}{dt} = \frac{V_{max,4,5}[dTDP]}{K_{m,4,5}\left(1 + \frac{[dTTP]+[dCDP]+[dCTP]}{K_{I,4,5}} + \frac{[dADP]+[dGDP]+[dATP]+[dGTP]}{K_{I,2,5}} + \frac{[ADP]+[ATP]}{K_{I,NDP}}\right) + [dTDP]} - \frac{0.75V_{max,4,5}[dTTP]}{K_{m,4,5}\left(1 + \frac{[dTDP]+[dCDP]+[dCTP]}{K_{I,4,5}} + \frac{[dADP]+[dGDP]+[dATP]+[dGTP]}{K_{I,2,5}} + \frac{[ADP]+[ATP]}{K_{I,NDP}}\right) + [dTTP]} + \frac{V_{max,4,7}[dTTP]_{cyto}}{K_{m,4,7}\left(1 + \frac{[dTDP]_{cyto}}{K_{I,4,6}} + \frac{[dCDP]_{cyto}}{K_{I,3,6}} + \frac{[dGDP]_{cyto}}{K_{I,2,6}} + \frac{[dADP]_{cyto}}{K_{I,1,6}} + \frac{[dCTP]_{cyto}}{K_{I,3,7}} + \frac{[dGTP]_{cyto}}{K_{I,2,7}} + \frac{[dATP]_{cyto}}{K_{I,1,7}}\right) + [dTTP]_{cyto}} - \frac{V_{max,4,7}[dTTP]}{K_{m,4,7}\left(1 + \frac{[dTDP]}{K_{I,4,6}} + \frac{[dCDP]}{K_{I,3,6}} + \frac{[dGDP]}{K_{I,2,6}} + \frac{[dADP]}{K_{I,1,6}} + \frac{[dCTP]}{K_{I,3,7}} + \frac{[dGTP]}{K_{I,2,7}} + \frac{[dATP]}{K_{I,1,7}}\right) + [dTTP]} - (R_{poly} \times fT) \quad (A4)$$

V_{max}, K_m, and K_i terms are shown in matrix format to specify the values in Table 2. Values for K_i terms not listed in matrix notation can be found by identifying the inhibitor in the middle column of Table 1.

REFERENCES

1. **Arner ES and Eriksson S.** Mammalian deoxyribonucleoside kinases. *Pharmacol Ther* 67: 155–186, 1995.
2. **Attardi G, Keeley B, and Tu C.** Photosensitivity and heat resistance conferred by BrdU incorporation upon a thymidine kinase-deficient mouse cell line with persistent mitochondrial enzyme activity. *J Cell Sci* 19: 55–68, 1975.
3. **Berk AJ and Clayton DA.** A genetically distinct thymidine kinase in mammalian mitochondria: exclusive labeling of mitochondrial deoxyribonucleic acid. *J Biol Chem* 248: 2722–2729, 1973.
4. **Bowmaker M, Yang MY, Yasukawa T, Reyes A, Jacobs HT, Huberman JA, and Holt IJ.** Mammalian mitochondrial DNA replicates bidirectionally from an initiation zone. *J Biol Chem* 278: 50961–50969, 2003.
5. **Camins A, Jiménez A, Sureda FX, Pallàs M, Escubedo E, and Camarasa J.** Characterization of nitrobenzylthioinosine binding sites in the mitochondrial fraction of rat testis. *Life Sci* 58: 753–759, 1996.
6. **Clayton DA.** Replication of animal mitochondrial DNA. *Cell* 28: 693–705, 1982.
7. **Cohen A, Barankiewicz J, Lederman HM, and Gelfand EW.** Purine and pyrimidine metabolism in human T lymphocytes: regulation of deoxyribonucleotide metabolism. *J Biol Chem* 258: 12334–12340, 1983.
8. **Collins A and Oates DJ.** Hydroxyurea: effects on deoxyribonucleotide pool sizes correlated with effects on DNA repair in mammalian cells. *Eur J Biochem* 169: 299–305, 1987.
9. **Copeland WC and Longley MJ.** DNA polymerase gamma in mitochondrial DNA replication and repair. *ScientificWorldJournal* 3: 34–44, 2003.
10. **Curbo S, Amiri M, Foroogh F, Johansson M, and Karlsson A.** The *Drosophila melanogaster* UMP-CMP kinase cDNA encodes an N-terminal mitochondrial import signal. *Biochem Biophys Res Commun* 311: 440–445, 2003.
11. **Das M, Parker JE, and Halestrap AP.** Matrix volume measurements challenge the existence of diazoxide/glibencamide-sensitive K_{ATP} channels in rat mitochondria. *J Physiol* 547: 893–902, 2003.
12. **Di Pierro D, Tavazzi B, Perno CF, Bartolini M, Balestra E, Calio R, Giardina B, and Lazzarino G.** An ion-pairing high-performance liquid chromatographic method for the direct simultaneous determination of nucleotides, deoxynucleotides, nicotinic coenzymes, oxypurines, nucleosides, and bases in perchloric acid cell extracts. *Anal Biochem* 231: 407–412, 1995.
13. **Dolce V, Fiermonte G, Runswick MJ, Palmieri F, and Walker JE.** The human mitochondrial deoxynucleotide carrier and its role in the toxicity of nucleoside antivirals. *Proc Natl Acad Sci USA* 98: 2284–2288, 2001.
14. **Elpeleg O, Mandel H, and Saada A.** Depletion of the other genome-mitochondrial DNA depletion syndromes in humans. *J Mol Med* 80: 389–396, 2002.
15. **Enríquez JA, Ramos J, Pérez-Martos A, López-Pérez MJ, and Montoya J.** Highly efficient DNA synthesis in isolated mitochondria from rat liver. *Nucleic Acids Res* 22: 1861–1865, 1994.
16. **Erent M, Gonin P, Cherfils J, Tissier P, Raschellà G, Giartosio A, Agou F, Sarger C, Lacombe ML, Konrad M, and Lascu I.** Structural and catalytic properties and homology modelling of the human nucleoside diphosphate kinase C, product of the *DRnm23* gene. *Eur J Biochem* 268: 1972–1981, 2001.
17. **Eriksson S, Arner E, Spasokoukotskaja T, Wang L, Karlsson A, Brosjo O, Gunven P, Julusson G, and Liliemark J.** Properties and levels of deoxynucleoside kinases in normal and tumor cells; implications for chemotherapy. *Adv Enzyme Regul* 34: 13–25, 1994.
18. **Eriksson S, Munch-Petersen B, Johansson K, and Eklund H.** Structure and function of cellular deoxyribonucleoside kinases. *Cell Mol Life Sci* 59: 1327–1346, 2002.
19. **Furman PA, Fyfe JA, St. Clair MH, Weinhold K, Rideout JL, Freeman GA, Lehrman SN, Bolognesi DP, Broder S, Mitsuya H, and Barry DW.** Phosphorylation of 3′-azido-3′-deoxythymidine and selective interaction of the 5′-triphosphate with human immunodeficiency virus reverse transcriptase. *Proc Natl Acad Sci USA* 83: 8333–8337, 1986.
20. **Gaillard RK, Barnard J, Lopez V, Hodges P, Bourne E, Johnson L, Allen MI, Condreay P, Miller WH, and Condreay LD.** Kinetic analysis of wild-type and YMDD mutant hepatitis B virus polymerases and effects of deoxyribonucleotide concentrations on polymerase activity. *Antimicrob Agents Chemother* 46: 1005–1013, 2002.
21. **Gao WY, Cara A, Gallo RC, and Lori F.** Low levels of deoxynucleotides in peripheral blood lymphocytes: a strategy to inhibit human immunodeficiency virus type 1 replication. *Proc Natl Acad Sci USA* 90: 8925–8928, 1993.
22. **Gear AR and Bednarek JM.** Direct counting and sizing of mitochondria in solution. *J Cell Biol* 54: 325–345, 1972.
23. **Glas U and Bahr GF.** Quantitative study of mitochondria in rat liver: dry mass, wet mass, volume, and concentration of solids. *J Cell Biol* 29: 507–523, 1966.
24. **Greger J and Fabianowska-Majewska K.** A distinctive activity of 5′-nucleotidase for dTMP in rat liver mitochondria. *Enzyme* 25: 26–32, 1980.
25. **Gross NJ, Getz GS, and Rabinowitz M.** Apparent turnover of mitochondrial deoxyribonucleic acid and mitochondrial phospholipids in the tissues of the rat. *J Biol Chem* 244: 1552–1562, 1969.
26. **Hall SW and Kuhn H.** Purification and properties of guanylate kinase from bovine retinas and rod outer segments. *Eur J Biochem* 161: 551–556, 1986.
27. **Harmenberg J.** Intracellular pools of thymidine reduce the antiviral action of acyclovir. *Intervirology* 20: 48–51, 1983.
28. **Henneré G, Becher F, Pruvost A, Goujard C, Grassi J, and Benech H.** Liquid chromatography-tandem mass spectrometry assays for intracellular deoxyribonucleotide triphosphate competitors of nucleoside antiretrovirals. *J Chromatogr B Analyt Technol Biomed Life Sci* 789: 273–281, 2003.
29. **Herrström Sjöberg A, Wang L, and Eriksson S.** Antiviral guanosine analogs as substrates for deoxyguanosine kinase: implications for chemotherapy. *Antimicrob Agents Chemother* 45: 739–742, 2001.
30. **Huang D, Zhang Y, and Chen X.** Analysis of intracellular nucleoside triphosphate levels in normal and tumor cell lines by high-performance liquid chromatography. *J Chromatogr B Analyt Technol Biomed Life Sci* 784: 101–109, 2003.
31. **Iacobazzi V, Ventura M, Fiermonte G, Prezioso G, Rocchi M, and Palmieri F.** Genomic organization and mapping of the gene (SLC25A19) encoding the human mitochondrial deoxynucleotide carrier (DNC). *Cytogenet Cell Genet* 93: 40–42, 2001.
32. **Jackson RC, Lui MS, Boritzki TJ, Morris HP, and Weber G.** Purine and pyrimidine nucleotide patterns of normal, differentiating, and regenerating liver and of hepatomas in rats. *Cancer Res* 40: 1286–1291, 1980.
33. **Jiménez A, Pubill D, Pallàs M, Camins A, Lladó S, Camarasa J, and Escubedo E.** Further characterization of an adenosine transport system in the mitochondrial fraction of rat testis. *Eur J Pharmacol* 398: 31–39, 2000.
34. **Johnson AA and Johnson KA.** Fidelity of nucleotide incorporation by human mitochondrial DNA polymerase. *J Biol Chem* 276: 38090–38096, 2001.
35. **Johnson AA, Tsai Y, Graves SW, and Johnson KA.** Human mitochondrial DNA polymerase holoenzyme: reconstitution and characterization. *Biochemistry* 39: 1702–1708, 2000.
36. **Kacser H and Burns JA.** The control of flux. *Symp Soc Exp Biol* 27: 65–104, 1973.
37. **Korhonen JA, Pham XH, Pellegrini M, and Falkenberg M.** Reconstitution of a minimal mtDNA replisome in vitro. *EMBO J* 23: 2423–2429, 2004.
38. **Kowluru A, Tannous M, and Chen HQ.** Localization and characterization of the mitochondrial isoform of the nucleoside diphosphate kinase in the pancreatic beta cell: evidence for its complexation with mitochondrial succinyl-CoA synthetase. *Arch Biochem Biophys* 398: 160–169, 2002.
39. **Lacombe ML, Milon L, Munier A, Mehus JG, and Lambeth DO.** The human Nm23/nucleoside diphosphate kinases. *J Bioenerg Biomembr* 32: 247–258, 2000.
40. **Lai Y, Tse CM, and Unadkat JD.** Mitochondrial expression of the human equilibrative nucleoside transporter 1 (hENT1) results in enhanced mitochondrial toxicity of antiviral drugs. *J Biol Chem* 279: 4490–4497, 2004.
41. **Lambeth DO, Mehus JG, Ivey MA, and Milavetz BI.** Characterization and cloning of a nucleoside-diphosphate kinase targeted to matrix of mitochondria in pigeon. *J Biol Chem* 272: 24604–24611, 1997.
42. **Lee LS and Cheng Y.** Human thymidylate kinase: purification, characterization, and kinetic behavior of the thymidylate kinase derived from chronic myelocytic leukemia. *J Biol Chem* 252: 5686–5691, 1977.
43. **Lim SE, Longley MJ, and Copeland WC.** The mitochondrial p55 accessory subunit of human DNA polymerase γ enhances DNA binding,

promotes processive DNA synthesis, and confers *N*-ethylmaleimide resistance. *J Biol Chem* 274: 38197–38203, 1999.
44. **Longley MJ, Nguyen D, Kunkel TA, and Copeland WC.** The fidelity of human DNA polymerase γ with and without exonucleolytic proofreading and the p55 accessory subunit. *J Biol Chem* 276: 38555–38562, 2001.
45. **Magnusson J, Orth M, Lestienne P, and Taanman JW.** Replication of mitochondrial DNA occurs throughout the mitochondria of cultured human cells. *Exp Cell Res* 289: 133–142, 2003.
46. **Maher AD, Kuchel PW, Ortega F, de Atauri P, Centelles J, and Cascante M.** Mathematical modelling of the urea cycle: a numerical investigation into substrate channelling. *Eur J Biochem* 270: 3953–3961, 2003.
47. **Marongiu ME, August EM, and Prusoff WH.** Effect of 3′-deoxythymidin-2′-ene (d4T) on nucleoside metabolism in H9 cells. *Biochem Pharmacol* 39: 1523–1528, 1990.
48. **Marti R, Nishigaki Y, Vila MR, and Hirano M.** Alteration of nucleotide metabolism: a new mechanism for mitochondrial disorders. *Clin Chem Lab Med* 41: 845–851, 2003.
49. **Martomo SA and Mathews CK.** Effects of biological DNA precursor pool asymmetry upon accuracy of DNA replication in vitro. *Mutat Res* 499: 197–211, 2002.
50. **Maybaum J, Klein FK, and Sadee W.** Determination of pyrimidine ribotide and deoxyribotide pools in cultured cells and mouse liver by high-performance liquid chromatography. *J Chromatogr* 188: 149–158, 1980.
51. **Mazzon C, Rampazzo C, Scaini MC, Gallinaro L, Karlsson A, Meier C, Balzarini J, Reichard P, and Bianchi V.** Cytosolic and mitochondrial deoxyribonucleotidases: activity with substrate analogs, inhibitors and implications for therapy. *Biochem Pharmacol* 66: 471–479, 2003.
52. **Mehus JG, Deloukas P, and Lambeth DO.** NME6: a new member of the nm23/nucleoside diphosphate kinase gene family located on human chromosome 3p21.3. *Hum Genet* 104: 454–459, 1999.
53. **Milon L, Rousseau-Merck MF, Munier A, Erent M, Lascu I, Capeau J, and Lacombe ML.** nm23-H4, a new member of the family of human nm23/nucleoside diphosphate kinase genes localised on chromosome 16p13. *Hum Genet* 99: 550–557, 1997.
54. **Munch-Petersen B, Cloos L, Tyrsted G, and Eriksson S.** Diverging substrate specificity of pure human thymidine kinases 1 and 2 against antiviral dideoxynucleosides. *J Biol Chem* 266: 9032–9038, 1991.
55. **Noma T, Fujisawa K, Yamashiro Y, Shinohara M, Nakazawa A, Gondo T, Ishihara T, and Yoshinobu K.** Structure and expression of human mitochondrial adenylate kinase targeted to the mitochondrial matrix. *Biochem J* 358: 225–232, 2001.
56. **Pak YK and Weiner H.** Import of chemically synthesized signal peptides into rat liver mitochondria. *J Biol Chem* 265: 14298–14307, 1990.
57. **Pastor-Anglada M, Casado FJ, Valdés R, Mata J, García-Manteiga J, and Molina M.** Complex regulation of nucleoside transporter expression in epithelial and immune system cells. *Mol Membr Biol* 18: 81–85, 2001.
58. **Pennycooke M, Chaudary N, Shuralyova I, Zhang Y, and Coe IR.** Differential expression of human nucleoside transporters in normal and tumor tissue. *Biochem Biophys Res Commun* 280: 951–959, 2001.
59. **Pillwein K, Jayaram HN, and Weber G.** Effect of ischemia on nucleosides and bases in rat liver and hepatoma 3924A. *Cancer Res* 47: 3092–3096, 1987.
60. **Pontarin G, Gallinaro L, Ferraro P, Reichard P, and Bianchi V.** Origins of mitochondrial thymidine triphosphate: dynamic relations to cytosolic pools. *Proc Natl Acad Sci USA* 100: 12159–12164, 2003.
61. **Raatikainen MJ, Peuhkurinen KJ, Kiviluoma KT, Hiltunen JK, and Hassinen IE.** 5′-Nucleotidase activity and adenosine production in rat liver mitochondria. *Biochim Biophys Acta* 1099: 238–246, 1992.
62. **Rampazzo C, Ferraro P, Pontarin G, Fabris S, Reichard P, and Bianchi V.** Mitochondrial deoxyribonucleotides, pool sizes, synthesis, and regulation. *J Biol Chem* 279: 17019–17026, 2004.
63. **Rampazzo C, Gallinaro L, Milanesi E, Frigimelica E, Reichard P, and Bianchi V.** A deoxyribonucleotidase in mitochondria: involvement in regulation of dNTP pools and possible link to genetic disease. *Proc Natl Acad Sci USA* 97: 8239–8244, 2000.
64. **Reichard P.** Interactions between deoxyribonucleotide and DNA synthesis. *Annu Rev Biochem* 57: 349–374, 1988.
65. **Robberson DL, Kasamatsu H, and Vinograd J.** Replication of mitochondrial DNA: circular replicative intermediates in mouse L cells. *Proc Natl Acad Sci USA* 69: 737–741, 1972.
66. **Rosenberg MJ, Agarwala R, Bouffard G, Davis J, Fiermonte G, Hilliard MS, Koch T, Kalikin LM, Makalowska I, Morton DH, Petty EM, Weber JL, Palmieri F, Kelley RI, Schäffer AA, and Biesecker LG.** Mutant deoxynucleotide carrier is associated with congenital microcephaly. *Nat Genet* 32: 175–179, 2002.
67. **Roy B, Beuneu C, Roux P, Buc H, Lemaire G, and Lepoivre M.** Simultaneous determination of pyrimidine or purine deoxyribonucleoside triphosphates using a polymerase assay. *Anal Biochem* 269: 403–409, 1999.
68. **Saada A, Shaag A, and Elpeleg O.** mtDNA depletion myopathy: elucidation of the tissue specificity in the mitochondrial thymidine kinase (TK2) deficiency. *Mol Genet Metab* 79: 1–5, 2003.
69. **Sampol J, Dussol B, Fenouillet E, Capo C, Mege JL, Halimi G, Bechis G, Brunet P, Rochat H, Berland Y, and Guieu R.** High adenosine and deoxyadenosine concentrations in mononuclear cells of hemodialyzed patients. *J Am Soc Nephrol* 12: 1721–1728, 2001.
70. **Snyder RD.** The role of deoxynucleoside triphosphate pools in the inhibition of DNA-excision repair and replication in human cells by hydroxyurea. *Mutat Res* 131: 163–172, 1984.
71. **Snyder RD and Davis GF.** Deoxynucleoside triphosphate pool perturbation is not a general feature in mutagen-treated mammalian cells. *Mutat Res* 209: 51–56, 1988.
72. **Song S, Wheeler LJ, and Mathews CK.** Deoxyribonucleotide pool imbalance stimulates deletions in HeLa cell mitochondrial DNA. *J Biol Chem* 278: 43893–43896, 2003.
73. **Tamiya N, Yusa T, Yamaguchi Y, Tsukifuji R, Kuroiwa N, Moriyama Y, and Fujimura S.** Co-purification of thymidylate kinase and cytosolic thymidine kinase from human term placenta by affinity chromatography. *Biochim Biophys Acta* 995: 28–35, 1989.
74. **Tomasselli AG and Noda LH.** Mitochondrial GTP-AMP phosphotransferase: 2. Kinetic and equilibrium dialysis studies. *Eur J Biochem* 93: 263–267, 1979.
75. **Tomasselli AG, Schirmer RH, and Noda LH.** Mitochondrial GTP-AMP phosphotransferase: 1. Purification and properties. *Eur J Biochem* 93: 257–262, 1979.
76. **Traut TW.** Physiological concentrations of purines and pyrimidines. *Mol Cell Biochem* 140: 1–22, 1994.
77. **Tsuiki H, Nitta M, Furuya A, Hanai N, Fujiwara T, Inagaki M, Kochi M, Ushio Y, Saya H, and Nakamura H.** A novel human nucleoside diphosphate (NDP) kinase, Nm23-H6, localizes in mitochondria and affects cytokinesis. *J Cell Biochem* 76: 254–269, 1999.
78. **Turner TE, Schnell S, and Burrage K.** Stochastic approaches for modelling in vivo reactions. *Comput Biol Chem* 28: 165–178, 2004.
79. **Valdés R, Casado FJ, and Pastor-Anglada M.** Cell-cycle-dependent regulation of CNT1, a concentrative nucleoside transporter involved in the uptake of cell-cycle-dependent nucleoside-derived anticancer drugs. *Biochem Biophys Res Commun* 296: 575–579, 2002.
80. **Walters RA, Tobey RA, and Ratliff RL.** Cell-cycle-dependent variations of deoxyribonucleoside triphosphate pools in Chinese hamster cells. *Biochim Biophys Acta* 319: 336–347, 1973.
81. **Wang L and Eriksson S.** Mitochondrial deoxyguanosine kinase mutations and mitochondrial DNA depletion syndrome. *FEBS Lett* 554: 319–322, 2003.
82. **Wang L, Saada A, and Eriksson S.** Kinetic properties of mutant human thymidine kinase 2 suggest a mechanism for mitochondrial DNA depletion myopathy. *J Biol Chem* 278: 6963–6968, 2003.
83. **Watkins LF and Lewis RA.** The metabolism of deoxyguanosine in mitochondria: characterization of the uptake process. *Mol Cell Biochem* 77: 71–77, 1987.
84. **Watkins LF and Lewis RA.** Phosphorylation of deoxyguanosine in intact and fractured mitochondria. *Mol Cell Biochem* 77: 153–160, 1987.
85. **Yang MY, Bowmaker M, Reyes A, Vergani L, Angeli P, Gringeri E, Jacobs HT, and Holt IJ.** Biased incorporation of ribonucleotides on the mitochondrial L-strand accounts for apparent strand-asymmetric DNA replication. *Cell* 111: 495–505, 2002.